Articles

Coordination of 2,2′-Bipyridyl and 1,10-Phenanthroline to Substituted Ytterbocenes: An Experimental Investigation of Spin Coupling in Lanthanide Complexes

Madeleine Schultz, James M. Boncella, David J. Berg, T. Don Tilley, and Richard A. Andersen*,[1]

Chemistry Department and Chemical Sciences Division of Lawrence Berkeley National Laboratory, University of California, Berkeley, California 94720

Received July 24, 2001

Addition of 2,2′-bipyridyl to diamagnetic $(Me_5C_5)_2Yb(OEt_2)$ gives the brown adduct $(Me_5C_5)_2Yb(bipy)$. The solution ^1H NMR and electronic absorption spectra show that the bipyridyl complex is paramagnetic, containing a bipyridyl radical anion, which can also be detected in the solid-state infrared spectrum and by the single-crystal X-ray crystallographic analysis. However, the measured magnetic moment, which varies from less than 1 μ_B at 5 K to 2.5 μ_B at 300 K, is higher than expected for $(Me_5C_5)_2Yb^{II}(bipy^0)$ and less than expected for $(Me_5C_5)_2Yb^{III}(bipy^-)$. An electron exchange model for spin coupling between Yb(III), with electron configuration $4f^{13}$, and the single unpaired electron in the bipyridyl radical anion is presented, based on comparison with the iodide salt $[(Me_5C_5)_2Yb^{III}(bipy^0)]^+[I]^-$. Comparing the magnetic susceptibility of $(Me_5C_5)_2Yb(phen)$ with its iodide salt shows similar behavior with phenanthroline as ligand. The extent of paramagnetism and therefore the exchange coupling is changed by the nature of the substituents on the cyclopentadienide rings; electron-withdrawing $SiMe_3$ groups favor Yb(II), while electron-donating alkyl groups stabilize the Yb(III) species. The molecular structures of many of the compounds have been determined in the solid state, and the bond distances and angles are consistent with the interpretation of the magnetism. The ring substituents, and therefore the different magnetic environments about the ytterbium center, also influence the rate of intermolecular exchange of the heterocyclic base ligands in solution; when the ligand is reduced, it exchanges more slowly than in the diamagnetic compounds.

Introduction

The bis-pyridine adduct of bis(pentamethylcyclopentadienyl)ytterbium, $(Me_5C_5)_2Yb(py)_2$, is a green, diamagnetic complex, as expected since Yb(II) has a closed shell, $5d^04f^{14}$ electronic structure.[2] The samarocene-bipyridyl adduct, $(Me_5C_5)_2Sm(bipy)$, has been postulated to be a Sm(III) complex of 2,2′-bipyridyl radical anion.[3] Given the lower oxidation potentials of ytterbium and europium compared with samarium, it was of interest to synthesize the analogous ytterbocene- and europocene-bipyridyl complexes to determine whether the bipyridyl ligand would be similarly reduced. The adducts of $(Me_5C_5)_2Yb$ with bipyridyl and 1,10-phenanthroline are stoichiometrically related to the bis-pyridine adduct, but their chemical and physical properties are different.

Several studies of ytterbium coordination complexes of bipyridyl show that the ligands are reduced. The first low-valent coordination complex of ytterbium, $Yb(bipy)_4$, was prepared over 30 years ago.[4,5] There is some dispute about the value and interpretation of the magnetic susceptibility of this complex and its phenanthroline analogue, but the electronic structure is not consistent with a zerovalent ytterbium center. A related complex, $Yb(Me_3CN(CH)_2NCMe_3)_3$, exhibits a temperature-dependent effective magnetic moment that has been interpreted in terms of an equilibrium between two complexes, $Yb(II)(L^-)_2(L)$ and $Yb(III)(L^-)_3$, the latter of which is favored at higher temperature.[6] Recently, the complex $Yb_3(bipy)_3(THF)_6$ has been isolated, in which each bipyridyl unit is dianionic and bridges two Yb(II) centers.[7] A review of bipyridyl radical anions and their role in metal complexes has appeared.[8]

(1) Address correspondence to the Chemistry Department, University of California, Berkeley, CA 94720; raandersen@lbl.gov.

(2) Tilley, T. D.; Andersen, R. A.; Spencer, B.; Zalkin, A. *Inorg. Chem.* **1982**, *21*, 2647−2649.

(3) Evans, W. J.; Drummond, D. K. *J. Am. Chem. Soc.* **1989**, *111*, 3329−3335.

(4) Feistel, G. R.; Mathai, T. P. *J. Am. Chem. Soc.* **1968**, *90*, 2988−2989.

(5) *Gmelin Handbook of Inorganic Chemistry, Sc, Y, La−Lu: Rare Earth Elements*, 8th ed.; Springer-Verlag: Berlin, 1980; Vol. D1.

(6) Bochkarev, A. A.; Trifonov, F. G.; Cloke, G. N.; Dalby, C. I.; Matsunaga, P. T.; Andersen, R. A.; Schumann, H.; Loebel, J.; Hemling, H. *J. Organomet. Chem.* **1995**, *486*, 177−182.

10.1021/om010661k CCC: $22.00
Publication on Web 12/29/2001

Table 1. Physical Characteristics of Metallocene Bipyridyl Complexes

complex	color	mp (°C)	IR (cm^{-1})[a]	μ_{eff} (300 K)[b]
$(Me_5C_5)_2Yb(bipy)$	red-brown	322−323	942, 1553	2.4 μ_B
$(Me_5C_5)_2Yb(dmb)$	red-brown	>330	944, 1595	2.4 μ_B
$(Me_5C_5)_2Yb(phen)$	dark blue	297−300	1610	4.0 μ_B
$[(Me_5C_5)_2Yb(bipy)]^+[I]^-$	red-brown	125−130	1595	4.2 μ_B
$[(Me_5C_5)_2Yb(bipy)]^+[(Me_5C_5)_2YbCl_2]^-$	red	264−266	1598	6.4 μ_B
$[(Me_5C_5)_2Yb(phen)]^+[I]^-$	red-brown	173−177	855	4.5 μ_B
$[1,3\text{-}(Me_3C)_2C_5H_3]_2Yb(bipy)$	blue-green	278−280	1593	diamagnetic
$[1,3\text{-}(Me_3C)_2C_5H_3]_2Yb(phen)$	dark blue	224−228	1615	3.4 μ_B
$[1,3\text{-}(Me_3Si)_2C_5H_3]_2Yb(bipy)$	green	208−212	1594	diamagnetic
$[1,3\text{-}(Me_3Si)_2C_5H_3]_2Yb(phen)$	red	216−218	830	diamagnetic
$(Me_4C_5H)_2Yb(bipy)$	red-brown	285−288	948, 1549	2.9 μ_B
$(Me_4C_5H)_2Yb(phen)$	purple	230−233	1612	4.2 μ_B
$(Me_5C_5)_2Ca(bipy)$[c]	orange-red	>330	1592, 1598	diamagnetic
$(Me_5C_5)_2Eu(bipy)$	red-brown	328−332	1591	7.4 μ_B

[a] Only relevant absorptions listed; see text for details. [b] Measured in the solid state. [c] Ref 16.

In this work, the synthesis and characterization of the complexes $(Me_5C_5)_2Yb(bipy)$, $(Me_5C_5)_2Eu(bipy)$, and $(Me_5C_5)_2Yb(phen)$ is described, as well as related compounds having differently substituted cyclopentadienide ligands. The spectroscopic and magnetic measurements on the compounds are interpreted in order to provide insight into the electronic structure of these molecules.

Results and Discussion

Synthesis. Addition of a toluene solution of 2,2′-bipyridyl to a toluene solution of $(Me_5C_5)_2Yb(OEt_2)$ results in an immediate color change from deep green to dark red-brown. Cooling this solution leads to the isolation of dark brown crystals of $(Me_5C_5)_2Yb(bipy)$ in high yield. The other complexes described here can be synthesized in a similar manner (eq 1).

$$Cp'_2Yb(OEt_2) + L \rightarrow Cp'_2YbL + OEt_2 \qquad (1)$$

Cp′ = Me_5C_5, 1,3-$(Me_3C)_2C_5H_3$, 1,3-$(Me_3Si)_2C_5H_3$, Me_4C_5H

L = 2,2′-bipyridyl (bipy), 4,4′-dimethyl-2,2′-bipyridyl (dmb), 1,10-phenanthroline (phen)

The solubility of the bipyridyl complexes in aromatic hydrocarbon solvents is relatively low, and that of the phenanthroline complexes is even lower. Not surprisingly, the melting points of the adducts are uniformly high; these and other physical characteristics of the complexes are collected in Table 1. It may be seen from Table 1 that $(Me_5C_5)_2Yb(bipy)$ is not diamagnetic at room temperature in the solid state as expected for an Yb(II) metallocene adduct, but the effective magnetic moment is less than that expected for an Yb(III)-radical anion complex, for which a value of 4.5−5 μ_B is predicted, as described in detail below.[9−11] The effective magnetic moment at room temperature for the phenanthroline adduct is substantially higher than that for the bipyridyl adduct, although still lower than the expected value. Further inspection of Table 1 shows that the room-temperature μ_{eff} values of the ytterbocene complexes range from diamagnetic to paramagnetic, depending on the substituents on the cyclopentadienide rings. The europocene complex has the expected magnetic moment for an Eu(II) center, showing that the bipyridyl ligand is not reduced in that case.

The reduction potentials of the pyridyl ligands used in this work are 2,2′-bipyridyl, −2.10 V; 4,4′-dimethyl-2,2′-bipyridyl, −2.15 V; 1,10-phenanthroline, −2.03 V, measured in anhydrous DMF and referred to SCE.[12,13] These values can be compared with the measured oxidation potentials of $(Me_5C_5)_2Yb$ and $(Me_5C_5)_2Eu$ in acetonitrile of +1.78 and +1.22 V vs Cp_2Fe/Cp_2Fe^+, which are equivalent to approximately +1.38 and +0.82 V vs SCE.[14] Thus, neither of these metallocenes is capable of reducing the heterocyclic bases. However, when the ligands bind to a metal, their reduction potentials are presumably lowered, as expected since the metal center is electropositive.

To provide comparisons for the spectroscopic and magnetic studies, the authentic Yb(III) metallocene bipyridyl cation was prepared with two different counterions, eqs 2 and 3. The Yb(III) metallocene phenanthroline cation was also prepared (eq 4).

$$(Me_5C_5)_2Yb(bipy) + AgI \rightarrow [(Me_5C_5)_2Yb(bipy)]^+[I]^- + Ag \qquad (2)$$

$$2(Me_5C_5)_2YbCl(THF) + bipy \rightarrow [(Me_5C_5)_2Yb(bipy)]^+[(Me_5C_5)_2YbCl_2]^- \qquad (3)$$

$$2(Me_5C_5)_2YbI + phen \rightarrow [(Me_5C_5)_2Yb(phen)]^+[I]^- \qquad (4)$$

The first of these complexes may be converted back to $(Me_5C_5)_2Yb(bipy)$ by reaction with sodium amalgam in THF. All three salts, which can be crystallized from dichloromethane, exhibit the expected effective magnetic moments at room temperature, Table 1.

(7) Fedushkin, I. L.; Petrovskaya, T. V.; Girgsdies, F.; Köhn, R. D.; Bochkarev, M. N.; Schumann, H. *Angew. Chem., Int. Ed.* **1999**, *38*, 2262−2264.
(8) Creutz, C. *Comments Inorg. Chem.* **1982**, *1*, 293−311.
(9) Berg, D. J.; Andersen, R. A.; Zalkin, A. *Organometallics* **1988**, *7*, 1858−1863.
(10) Berg, D. J.; Burns, C. J.; Andersen, R. A.; Zalkin, A. *Organometallics* **1989**, *8*, 1865−1870.
(11) Note that all magnetic susceptibility results have been acquired on several separate, analytically pure, samples of each compound that were prepared separately from different batches of starting material, over a time frame of several years.
(12) Saji, T.; Aoyagui, S. *Electroanal. Chem. Interfac. Electrochem.* **1975**, *58*, 401−410.
(13) Tabner, B. J.; Yandle, J. R. *J. Chem. Soc. A* **1968**, 381−388.
(14) Finke, R. G.; Keenan, S. R.; Schiraldi, D. A.; Watson, P. L. *Organometallics* **1986**, *5*, 598−601.

Characterization. Solid-State Measurements: Infrared Spectroscopy. The infrared spectrum of 2,2′-bipyridyl as a neutral and reduced ligand has been studied extensively,[15] enabling the oxidation state of this ligand to be inferred from infrared spectroscopy. Two key features have been noted; a strong absorbance is expected for bipyridyl radical anion in the region 900−1000 cm^{-1}, due to ring deformation modes of the ligand, and the 1475−1625 cm^{-1} region, where the C═C and C═N stretching motions of the bipyridyl ligand are expected. Thus, Nakamoto and co-workers classify bipyridyl ligands as neutral if they have no strong absorption between 900 and 1000 cm^{-1} and a strong band around 1600 cm^{-1}. When the ligand is reduced, a strong absorption in the 900−1000 cm^{-1} region and several strong to medium intensity bands in the 1575−1490 cm^{-1} region are observed. Table 1 includes only the bands in those regions for the molecules described here.

The infrared spectrum of $(Me_5C_5)_2Yb(bipy)$ contains an absorption at 942 cm^{-1}, while the infrared spectrum of $(Me_5C_5)_2Yb(dmb)$ has a similar absorption at 944 cm^{-1}, which identifies the ligand as the reduced radical anion in these two complexes. These two molecules also have bands at 1553 and 1595 cm^{-1}, respectively. Similarly, $(Me_4C_5H)_2Yb(bipy)$ has absorptions at 948 and 1549 cm^{-1}. The complexes $[1,3\text{-}(Me_3C)_2C_5H_3]_2Yb(bipy)$ and $[1,3\text{-}(Me_3Si)_2C_5H_3]_2Yb(bipy)$ do not have absorptions in the range 800−1000 cm^{-1} in their infrared spectra; instead they each have an absorption at 1594 cm^{-1}, identifying the bipyridyl ligand as neutral in these two adducts.

The cationic complexes $[(Me_5C_5)_2Yb(bipy)]^+[I]^-$ and $[(Me_5C_5)_2Yb(bipy)]^+[(Me_5C_5)_2YbCl_2]^-$ have strong absorptions at 1595 and 1598 cm^{-1}, respectively, while the europium and calcium complexes $(Me_5C_5)_2Eu(bipy)$ and $(Me_5C_5)_2Ca(bipy)$[16] also have absorptions in their infrared spectra at 1591 and 1592 cm^{-1}, respectively. None of these complexes have any absorbance in the region 800−1000 cm^{-1}. The infrared data are thus consistent with the bipyridyl ligand being neutral in these four adducts, as expected.

Since no systematic study of the infrared spectra of phenanthroline complexes has been published, there are no infrared criteria for deducing the nature of the phenanthroline ligand. However, bands in the region around 1600 cm^{-1} are observed for the ytterbocene phenanthroline complexes $(Me_5C_5)_2Yb(phen)$, $[1,3\text{-}(Me_3C)_2C_5H_3]_2Yb(phen)$, and $(Me_4C_5H)_2Yb(phen)$, but not for $[1,3\text{-}(Me_3Si)_2C_5H_3]_2Yb(phen)$ and $[(Me_5C_5)_2Yb(phen)]^+[I]^-$. The former, which is the only diamagnetic phenanthroline complex studied here, has a very intense absorbance at 830 cm^{-1} that is not observed in the other phenanthroline complexes. The cationic complex has a strong absorption at 855 cm^{-1}, so it seems reasonable to suggest that a band in this region may be characteristic of the neutral phenanthroline ligand, while an absorption near 1600 cm^{-1} may be characteristic of the reduced phenanthroline ligand.

Solid-State Measurements: X-ray Crystallography. In this work, the structures of the bipyridyl complexes $(Me_5C_5)_2Yb(bipy)$ and $[(Me_5C_5)_2Yb(bipy)]^+[(Me_5C_5)_2YbCl_2]^-$ were determined at room temperature, while the structure of $[1,3\text{-}(Me_3C)_2C_5H_3]_2Yb(bipy)$ was determined at low temperature. ORTEP diagrams for these three complexes are shown in Figures 1, 2, and 3, respectively, while Tables 2 and 3 present some important bond lengths and angles, and Table 4 contains selected data collection and structure solution parameters.

The X-ray crystal structures of bipyridyl complexes have been used as evidence for the oxidation state of the bipyridyl ligand, because donation of electron density into the LUMO of bipyridyl causes systematic changes to the bond lengths.[7,17] The LUMO of bipyridyl

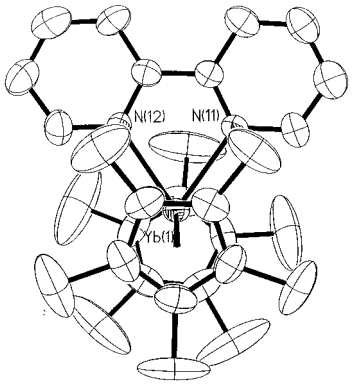

Figure 1. ORTEP diagram of $(Me_5C_5)_2Yb(bipy)$ showing one of the two unique molecules in the unit cell (50% probability ellipsoids).

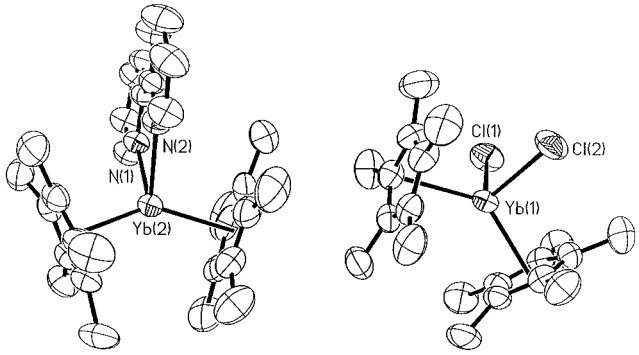

Figure 2. ORTEP diagram of $[(Me_5C_5)_2Yb(bipy)]^+[(Me_5C_5)_2YbCl_2]^-$ (50% probability ellipsoids).

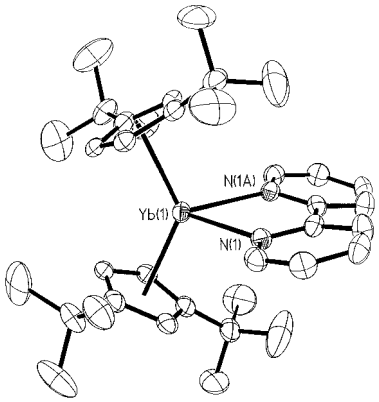

Figure 3. ORTEP diagram of $[1,3\text{-}(Me_3C)_2C_5H_3]_2Yb(bipy)\cdot$ toluene (50% probability ellipsoids) showing torsion of 2,2′-bipyridyl ligand. The toluene molecule has been omitted for clarity.

(15) Saito, Y.; Takemoto, J.; Hutchinson, B.; Nakamoto, K. *Inorg. Chem.* **1972**, *11*, 2003−2011.
(16) Burns, C. J.; Andersen, R. A. *J. Organomet. Chem.* **1987**, *325*, 31−37.

Table 2. Bond Distances (Å) of 2,2′-Bipyridyl from X-ray Crystallography

bond	free bipy[17]	$(Me_5C_5)_2Yb(bipy)$	$[(Me_5C_5)_2Yb(bipy)]^+[(Me_5C_5)_2YbCl_2]^-$	$[1,3\text{-}(Me_3C)_2C_5H_3]_2Yb(bipy)\cdot$toluene
A	1.490(3)	1.434	1.492(4)	1.48(1)
B	1.394(2)	1.419	1.385	1.392(8)
C	1.385(2)	1.387	1.380	1.386(9)
D	1.383(3)	1.420	1.370	1.376(8)
E	1.384(2)	1.398	1.370	1.369(8)
F	1.341(2)	1.358	1.339	1.338(8)
G	1.346(2)	1.383	1.343	1.351(7)

Table 3. Selected Bond Distances (Å) and Angles (deg) of $(Me_5C_5)_2Yb(bipy)$, $[(Me_5C_5)_2Yb(bipy)]^+[(Me_5C_5)_2YbCl_2]^-$, $[1,3\text{-}(Me_3C)_2C_5H_3]_2Yb(bipy)\cdot$toluene, $[1,3\text{-}(Me_3Si)_2C_5H_3]_2Yb(phen)$, and $[(Me_5C_5)_2Yb(phen)]^+[I]^-\cdot CH_2Cl_2$

	$(Me_5C_5)_2Yb(bipy)$	$[(Me_5C_5)_2Yb(bipy)]^+$ $[(Me_5C_5)_2YbCl_2]^-$	$[1,3\text{-}(Me_3C)_2C_5H_3]_2$-Yb(bipy)·toluene	$[1,3(Me_3Si)_2C_5H_3]_2$-Yb(phen)	$[(Me_5C_5)_2Yb(phen)]^+$ $[I]^-\cdot CH_2Cl_2$
M−C(ring) (mean)	2.62	2.59	2.75	2.72	2.605
M−Cp (mean)	2.34	2.30	2.468	2.43	2.31
Cp−M−Cp	139.3	141.5	131.6	130.9	141.1
M−N (mean)	2.32	2.37	2.503(4)	2.50	2.36
bond A	1.426(5)	1.492(4)	1.48(1)	1.422(7)	1.46(1)
torsion angle N−C−C−N	3	7	15	5	2
torsion angle C−C−C−C	3	8	19	3	1

Table 4. Selected Crystal Data and Data Collection Parameters for $(Me_5C_5)_2Yb(bipy)$, $[(Me_5C_5)_2Yb(bipy)]^+[(Me_5C_5)_2YbCl_2]^-$, $[1,3\text{-}(Me_3C)_2C_5H_3]_2Yb(bipy)\cdot$toluene, $[1,3\text{-}(Me_3Si)_2C_5H_3]_2Yb(phen)$, and $[(Me_5C_5)_2Yb(phen)]^+[I]^-\cdot CH_2Cl_2$

formula	$YbN_2C_{30}H_{38}$	$Yb_2Cl_2N_2C_{50}H_{68}$	$YbN_2C_{43}H_{58}$	$YbSi_4N_2C_{34}H_{50}$	$YbCl_4IN_2C_{34}H_{42}$
fw	599.68	1114.07	775.97	772.16	920.5
space group	*Pbca* (#61)	$P\bar{1}$ (#2)	*Fddd* (#70)	$P2_1/n$ (#14)	$P2_1/n$ (#14)
a (Å)	16.976(1)	10.8462(9)	19.3445(4)	11.2208(2)	14.3923(2)
b (Å)	30.060(5)	13.431(2)	24.4600(5)	19.2665(1)	14.6609(4)
c (Å)	21.255(3)	16.422(2)	30.1051(4)	17.9251(1)	17.4018(3)
α (deg)	90	90.61(1)	90	90	90
β (deg)	90	93.988(8)	90	104.796(1)	100.925(1)
γ (deg)	90	95.60(1)	90	90	90
V (Å^3)	10846.4	2380.6	14244.7(4)	3746.65(6)	3605.3(1)
Z	16	2	16	4	4
d_{calc} (g/cm^3)	1.469	1.554	1.451	1.369	1.70
μ(Mo Kα)$_{calc}$ (cm^{-1})	34.56	40.40	26.59	26.48	37.72
size (mm)	0.24 × 0.20 × 0.16	0.43 × 0.17 × 0.15	0.27 × 0.10 × 0.05	0.29 × 0.08 × 0.05	0.25 × 0.12 × 0.09
temperature (K)	298	298	138	138	151
diffractometer[a]	CAD-4	CAD-4	SMART	SMART	SMART
scan type, range	$\theta - 2\theta$, 3−45°	$\theta - 2\theta$, 3−45°	ω, 3−49.3°	ω, 3−46.5°	ω, 3−46.6°
no. of reflns collected	7780	6620	16 914	15 300	16 716
no. of unique reflns	7081	6223	3264	5550	5383
no. of reflns, $F_o^2 > 3\sigma(F_o^2)$	4494	5140	1726	3199	2985
variables	595	506	195	370	380
abs corr	Gaussian	Gaussian	empirical	empirical	empirical
transmn range	0.66−0.56	0.622−0.509	0.962−0.732	0.945−0.707	0.962−0.744
R[b]	0.033	0.023	0.025	0.024	0.034
R_w	0.034	0.026	0.025	0.024	0.035
R_{all}	0.092	0.032	0.032	0.059	0.041
GOF	1.653	1.719	0.75	0.73	1.08

[a] Radiation: graphite monochromated Mo Kα (λ = 0.71073 Å). [b] $R = \sum||F_o| - |F_c||/\sum|F_o|$.

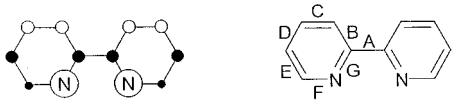

Figure 4. Schematic diagram showing the symmetry of the LUMO of 2,2′-bipyridyl, and diagram showing bond labeling scheme.

is represented in Figure 4 along with a diagram showing the bond-labeling scheme used in the following discussion.[18] It can be seen that upon acceptance of an electron into the LUMO, the bonds A, C, and E are expected to shorten, while the bonds B, D, F, and G are expected to lengthen. Table 2 compares the metrical parameters of bipyridyl in the structures with those of free bipyridyl. On the basis of the bond distances within the ligand, the bipyridyl ligand appears to be reduced in $(Me_5C_5)_2$-Yb(bipy), but neutral in the other two complexes.

Acceptance of an electron into the LUMO shown in Figure 4 is also expected to flatten the bipyridyl ligand as it gives double-bond character to the bond A. Conversely, if a bipyridyl ligand in a complex has a high torsion angle between the two pyridyl rings, this is an indication that the ligand is neutral in that complex. From Table 3 and Figures 1, 2, and 3, it can be seen

(17) Chisholm, M. H.; Huffman, J. C.; Rothwell, I. P.; Bradley, P. G.; Kress, N.; Woodruff, W. H. *J. Am. Chem. Soc.* **1981**, *103*, 4945−4947.

(18) McPherson, A. M.; Fieselmann, B. F.; Lichtenberger, D. L.; McPherson, G. L.; Stucky, G. D. *J. Am. Chem. Soc.* **1979**, *101*, 3425−3430.

that the bipyridyl ligand is planar in the molecule $(Me_5C_5)_2Yb(bipy)$ but not planar in the other two bipyridyl complexes. The pyridyl rings of $[1,3\text{-}(Me_3C)_2C_5H_3]_2Yb(bipy)$ are twisted with respect to each other, with a torsion angle of 17°. It is conceivable that the steric bulk of the disubstituted cyclopentadienide rings is causing this twist, which prevents electron transfer to the LUMO of bipyridyl and results in a neutral molecule. However, the pyridyl rings are each twisted toward, rather than away from, the nearest Me_3C group on the cyclopentadienide rings, indicating that the twist is not the result of steric hindrance to planarity. Were the ligand to be reduced and the metal oxidized, it would cause a decrease in the ionic radius of the metal from 1.14 to 0.985 Å.[19] This would result in a reduction in the metal−cyclopentadienide distance, which may cause unfavorable interactions between the Me_3C groups at the backside of the metallocene wedge. Thus, steric factors may be at work to prevent electron transfer from the metal to the ligand in this molecule.

Table 3 contains other important bond distances and angles for these molecules. The distance from a ligand to a metal is correlated with the oxidation state of the metal, as the ionic radius is smaller in a higher oxidation state.[19] Examination of the mean metal−ring carbon distance, the metal−centroid distance, and the metal−nitrogen distance indicates that in $(Me_5C_5)_2Yb(bipy)$ and $[(Me_5C_5)_2Yb(bipy)]^+[(Me_5C_5)_2YbCl_2]^-$ the ytterbium atom is Yb(III) while in $[1,3\text{-}(Me_3C)_2C_5H_3]_2Yb(bipy)$ it is Yb(II), consistent with the oxidation state as determined from the metrical parameters of the bipyridyl ligand. These values can also be compared with the corresponding values for $(Me_5C_5)_2Yb(py)_2$, in which the metal is divalent.[2] In that molecule, the mean metal−ring carbon distance is 2.74 Å and the mean metal−nitrogen distance is 2.56 Å.

The structures of the phenanthroline complexes $[1,3\text{-}(Me_3Si)_2C_5H_3]_2Yb(phen)$ and $[(Me_5C_5)_2Yb(phen)]^+[I]^-$ were also determined by X-ray crystallography at low temperature, and important bond lengths and angles are contained in Table 3, while Table 4 contains data collection and structure solution details. In the former molecule, the distances from the metal to its ligands indicate that the metal is in the divalent oxidation state (Table 3). The structure of this molecule is somewhat unexpected, in that the phenanthroline ligand does not lie on the plane bisecting the metallocene wedge. Instead, it forms an angle of 15° to that plane (Figure 5). This feature is most reasonably associated with the steric hindrance caused by the Me_3Si groups on the disubstituted cyclopentadienide rings. Unlike bipyridyl, the phenanthroline ligand cannot twist, so avoidance of the Me_3Si groups results in a tilted conformation.

The structure of the cationic complex $[(Me_5C_5)_2Yb(phen)]^+[I]^-$ was determined for comparison with the neutral compound and with the cationic bipyridyl complex (Figure 6). The iodide counterion is located more than 3.9 Å from the nearest carbon atom, and the molecule consists of discrete metallocene cations and iodide anions. In this compound, the phenanthroline ligand lies, as expected, on the plane bisecting the metallocene wedge. The distances and angles about the ytterbium center (Table 3) confirm that the metal is in the trivalent oxidation state.

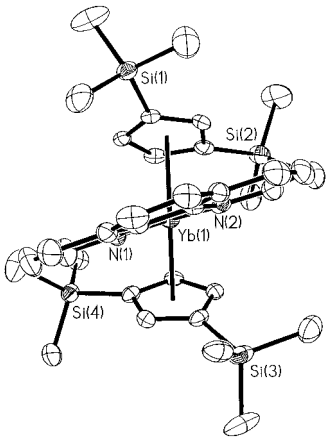

Figure 5. ORTEP diagram of $[1,3\text{-}(Me_3Si)_2C_5H_3]_2Yb(phen)$ (50% probability ellipsoids) showing twist of 1,10-phenanthroline ligand.

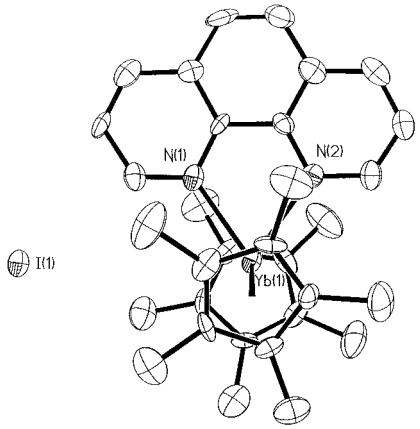

Figure 6. ORTEP diagram of $[(Me_5C_5)_2Yb(phen)]^+[I]^-$ (50% probability ellipsoids).

Solid-State Magnetic Measurements: SQUID. Trivalent ytterbium is a paramagnetic $4f^{13}$ ion. In a low-symmetry ligand field, the $^2F_{7/2}$ free ion ground state[20] is split into four Kramer's doublets.[21] At low temperatures, only the two lowest levels are likely to be populated and contribute to the magnetic moment. As a result, at temperatures from 5 to 30 K, a Yb(III) complex follows the Curie law ($C = \chi T$) with $\mu = 3.8\ \mu_B$. At temperatures above 30 K, thermal population of the third and fourth doublet levels becomes increasingly significant and the contribution of these levels to the magnetic moment results in deviation from Curie law behavior. By 90 K, both upper levels are easily accessible, while the next manifold of states, arising from the $^2F_{5/2}$ term, is 10 300 cm^{-1} higher in energy in the free ion and is not thermally accessible. Thus from 90 to 300 K, the temperature dependence of the magnetic susceptibility follows the Curie−Weiss law ($C = \chi(T - \theta)$) with a predicted $\mu = 4.5\ \mu_B$, which can be calculated from the term $^2F_{7/2}$.[20] This prediction is remarkably accurate for many Yb(III) salts.[21,22] The value of θ is typically −20 to −50 K. A plot of the inverse molar

(19) Shannon, R. D. *Acta Crystallogr., Sect. A* **1976**, *A32*, 751−767.
(20) Gerloch, M.; Constable, E. C. *Transition Metal Chemistry*; VCH: Weinheim, 1995.
(21) Boudreaux, E. A.; Mulay, L. N. *Theory and Applications of Molecular Paramagnetism*; Wiley-Interscience: New York, 1976.
(22) van Vleck, J. H. *The Theory of Electric and Magnetic Susceptibilities*; Clarendon Press: Oxford, 1932.

susceptibility ($1/\chi$) as a function of temperature for a typical Yb(III) compound therefore has two linear regions. The slope ($1/C$) of each region is directly related to the magnetic moment as $\mu = 2.828C^{1/2}$.[10]

For a complex containing two noninteracting spins, the contributions of the spins to the molar magnetic susceptibility are additive and the expected moment can be calculated as follows. The total susceptibility, χ_T, is the sum of the individual susceptibilities, $\chi_T = \chi_1 + \chi_2$, and so $\chi_T T = \chi_1 T + \chi_2 T$. The square of the effective magnetic moment is $\mu^2 = (2.828)^2(\chi T)$, so $\mu_T^2 = \mu_1^2 + \mu_2^2$, and the effective magnetic moment is then the square root of the sum of the squares of the individual moments, $\mu_T = (\mu_1^2 + \mu_2^2)^{1/2}$. Specifically, for an organoytterbium complex containing a reduced bipyridyl or phenanthroline ligand, in a situation where the ytterbium and radical anion spins are noninteracting, the predicted magnetic moment is therefore $((3.8)^2 + (1.73)^2)^{1/2} = 4.2\ \mu_B$ from about 5 to 30 K and $((4.5)^2 + (1.73)^2)^{1/2} = 4.8\ \mu_B$ from about 90 to 300 K.

The above calculation is not valid for a molecule in which the unpaired spins are coupled. Hatfield and coworkers have studied lanthanide−phthalocyaninato complexes in which exchange coupling is postulated.[23] For a system involving electron exchange coupling, the new term symbols can be calculated on the basis of linear combinations of the $^2F_{7/2}$ term of ytterbium and the $^2S_{1/2}$ term of the radical. For an antiferromagnetic interaction, this new term is $^{2S}L_{J-1/2} = {}^1F_3$, while for a ferromagnetic interaction the new term is $^{2S+2}L_{J+1/2} = {}^3F_4$. The predicted low and high limiting values for the room-temperature moment of Yb(III), antiferro- or ferromagnetically coupled with an organic radical, can then be calculated from these new term symbols; $^1F_3$ implies $\mu = 3.46\ \mu_B$ while $^3F_4$ gives $\mu = 5.59\ \mu_B$. Thus, whether coupling occurs, the magnetic moment of a complex containing Yb(III) and an organic radical should lie in the range 3.4−5.6 μ_B. Note that strong antiferromagnetic coupling in this system corresponds to a molecule with no formally unpaired spins, and the magnetism is attributed solely to orbital angular momentum. The experimental value of the room-temperature moment of $Yb(pc)_2$ (pc = phthalocyanine) is 4.3 μ_B, and the authors conclude that this molecule exhibits both the antiferro- and ferromagnetically coupled states of the ytterbium and phthalocyanine radical electrons.[23]

Magnetic measurements have been made on the complexes described here from 5 to 300K at low and high magnetic fields (5 and 40 kG). Plots of $1/\chi$ vs T and μ vs T for $[(Me_5C_5)_2Yb(bipy)]^+[(Me_5C_5)_2YbCl_2]^-$ are shown in Figure 7. It can be seen that the $1/\chi$ vs T curve for this salt follows the expected shape for two noninteracting Yb(III) centers, as it has two linear regions with gradients (μ) of $((3.8)^2 + (3.8)^2)^{1/2} = 5.4\ \mu_B$ at low temperature and $((4.5)^2 + (4.5)^2)^{1/2} = 6.4\ \mu_B$ at high temperature. These are the expected magnetic moments for a compound containing two isolated Yb(III) paramagnets.[10] Figure 8 shows the $1/\chi$ vs T and μ vs T plots for $(Me_5C_5)_2Yb(bipy)$. Clearly, the shape of the $1/\chi$ vs T curve and the magnetic moment are very different from those expected for an isolated Yb(III) paramagnet and a radical anion. These data are interpreted in detail

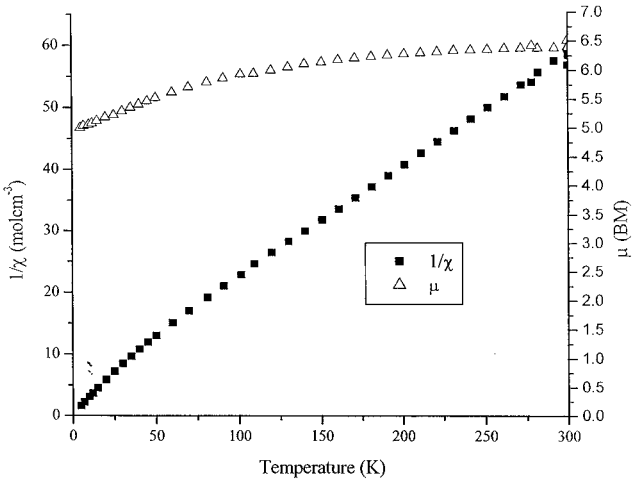

Figure 7. Thermal dependence of μ and $1/\chi$ for $[(Me_5C_5)_2Yb(bipy)]^+[(Me_5C_5)_2YbCl_2]^-$ at 5 kG.

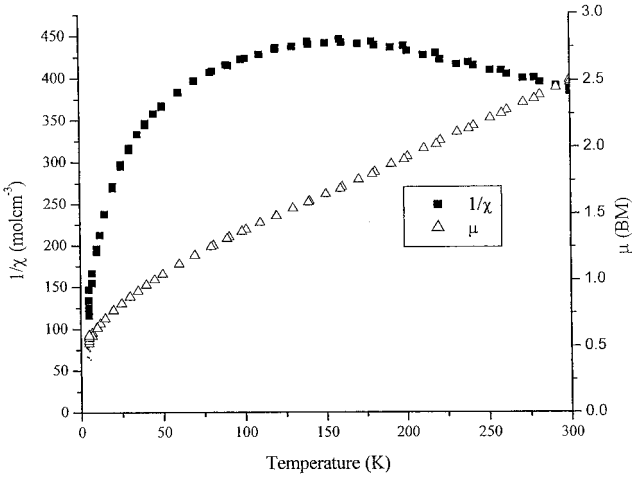

Figure 8. Thermal dependence of μ and $1/\chi$ for $(Me_5C_5)_2Yb(bipy)$ at 5 and 40 kG.

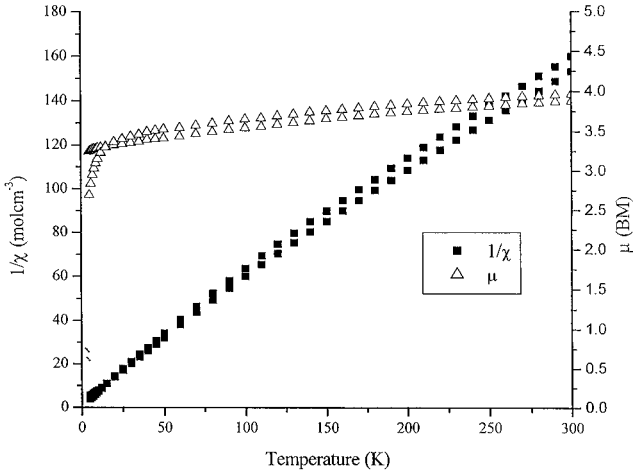

Figure 9. Thermal dependence of μ and $1/\chi$ for $(Me_5C_5)_2Yb(phen)$ at 5 and 40 kG.

below. Variable-temperature magnetic susceptibility measurements of the 1,10-phenanthroline adducts of $(Me_5C_5)_2Yb$, $[1,3\text{-}(Me_3C)_2C_5H_3]_2Yb$, and $(Me_4C_5H)_2Yb$ show that the shapes of their $1/\chi$ vs T plots are normal, but the values of μ are lower than expected. Figure 9 shows the $1/\chi$ vs T and μ vs T plots for $(Me_5C_5)_2Yb(phen)$; the other two phenanthroline adducts have

(23) Trojan, K. L.; Kendall, J. L.; Kepler, K. D.; Hatfield, W. E. *Inorg. Chim. Acta* **1992**, *198−200*, 795−803.

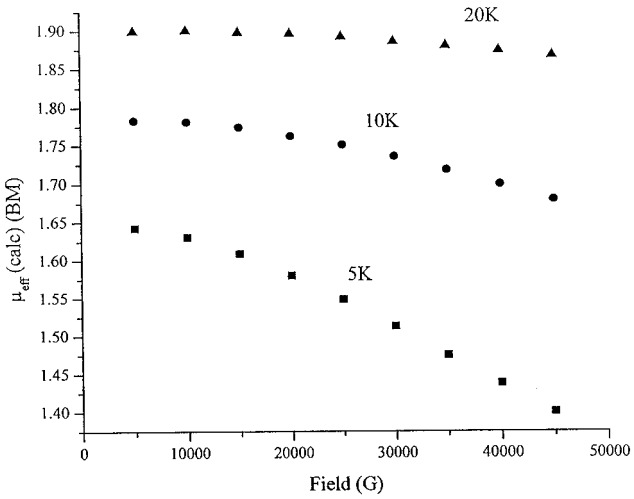

Figure 10. Field dependence of μ for $(Me_5C_5)_2Yb(bipy)$ at 5, 10, and 20 K.

similar curve shapes and resulting magnetic moments. At 300 K, the effective magnetic moment of 3.4 μ_B for $[1,3\text{-}(Me_3C)_2C_5H_3]_2Yb(phen)$ is very close to the value predicted for antiferromagnetic coupling of the two spins as described above. The values of the effective moments for the other two phenanthroline adducts are higher, 3.8−to 4.2 μ_B, and close to the value found by Hatfield for $Yb(pc)_2$ of 4.3 μ_B, which was attributed to the presence of both ferro- and antiferromagnetically coupled states of Yb(III) and the radical anion.[23]

In contrast, the shapes of the $1/\chi$ vs T and μ vs T plots for $(Me_5C_5)_2Yb(bipy)$ shown in Figure 8 are unusual and clearly different from that described in the preceding paragraphs. The SQUID data for $(Me_5C_5)_2Yb(dmb)$ and $(Me_4C_5H)_2Yb(bipy)$ are virtually superimposable over that for $(Me_5C_5)_2Yb(bipy)$. As can be seen in Figure 8, the $1/\chi$ vs T plot is nonlinear and has a maximum value, corresponding to a minimum value of χ, at 150 K. The plot of μ vs T indicates that the effective magnetic moment of the sample increases monotonically from 0.5 μ_B at 5 K to 2.4 μ_B at 300 K, and a value in the expected range (3.4−5.6 μ_B) has not been reached at room temperature. It can be seen from the divergence of the data at the two fields used in Figure 8 that the magnetic moment of $(Me_5C_5)_2Yb(bipy)$ is also field dependent at low temperatures. Its magnetization was therefore examined as a function of the applied field at temperatures of 5, 10, and 20 K (Figure 10). At 5 K, the effective moment becomes smaller as the field is increased, while above 20 K the moment is field-independent. These measurements show that antiferromagnetic coupling is occurring at low temperatures, because when a stronger field is applied, more spins are aligned and the effective moment is lower. The overall moment becomes higher as the temperature increases, due to population of higher spin states as described above, and the moment becomes field independent. Similar observations were made for $(Me_5C_5)_2Yb(phen)$, consistent with the qualitative notion of antiferromagnetic alignment of the two spins.

The solid-state magnetic susceptibilities of the two adducts, $(Me_5C_5)_2Yb(bipy)$ and $(Me_5C_5)_2Yb(phen)$, clearly cannot be described by a model in which the spin carriers are uncorrelated; the μ values are far too low. No theoretical model is currently available for quantum mechanical electron exchange coupling in f-transition metals.[24] However, Kahn has persuasively argued an experimental model for handling the electron exchange between the spin carriers in a coordination complex of a trivalent lanthanide metal ion in which the ligand is a radical, and Costes has also used a similar empirical approach.[25,26] The experimental model involves expressing the temperature dependence of the magnetic susceptibility in a χT vs T plot. The corresponding data are collected for an isostructural complex in which the ligand is diamagnetic. Subtracting these two curves yields a $\Delta\chi T$ vs T plot, the slope of which shows whether the spin carriers interact in a ferro- or antiferromagnetic manner.[26] This subtraction procedure deals with the spin−orbit coupling problem since the crystal field around the lanthanide ion, and therefore the population of the Kramer's doublets, in each case can be assumed to be identical. The value of the coupling constant cannot be obtained, but its sign, that is, whether the interaction is ferro- or antiferromagnetic, can be determined in this manner.

Kahn's methodology may be applied to $(Me_5C_5)_2Yb(bipy)$ and $(Me_5C_5)_2Yb(phen)$, since the iodide salts are known and the variable-temperature magnetic susceptibilities have been measured. The neutral adducts contain Yb(III) and a radical, while the salts contain Yb(III) and a diamagnetic ligand. The geometries of the fragments are likely to be identical; the structure of $[(Me_5C_5)_2Yb(bipy)]^+[I]^-$ is not available, as suitable single crystals could not be grown, but that of the cationic fragment of the salt $[(Me_5C_5)_2Yb(bipy)]^+[(Me_5C_5)_2YbCl_2]^-$ is very similar to that of the neutral adduct (Figures 1 and 2 and Table 3). In the case of the phenanthroline complexes, although the structure of $(Me_5C_5)_2Yb(phen)$ could not be determined, the geometric parameters are expected to be similar to those of $(Me_5C_5)_2Yb(bipy)$, which in turn is similar to $[(Me_5C_5)_2Yb(phen)]^+[I]^-$ (Figures 1 and 6 and Table 3). The similarity of the geometrical parameters supports the notion that the environment and therefore crystal fields around the Yb atoms are very similar in the two pairs of complexes. The χT vs T plots at 40 kG are shown in Figures 11 and 12 for the phenanthroline and bipyridyl adducts, respectively. The χT vs T plot for $[(Me_5C_5)_2Yb(phen)]^+[I]^-$ is as expected for an isolated Yb(III) paramagnet. At 300K, χT has a value of 2.6 $cm^3\ mol^{-1}\ K^{-1}$, and the expected value for a $^2F_{7/2}$ state is 2.57. The value of χT is independent of temperature from 300 K down to about 150 K and then decreases with decreasing temperature due to the changing population of Kramer's doublet states. The χT vs T plot for $(Me_5C_5)_2Yb(phen)$ shows χT decreasing from a value of 1.9 $cm^3\ mol^{-1}\ K^{-1}$ at 300 K, which is much lower than the expected value of 2.94 for two uncorrelated spins. Subtraction of these two curves yields the $\Delta\chi T$ vs T plot, which increases slightly with decreasing temperature from 300 to 100 K, then decreases, indicating that the ground state is antiferromagnetically coupled.[26] Representing the data in this way unequivocally shows that the spin carriers

(24) Edelstein, N. *Electronic Structure and Optical Spectroscopy of f^n Ions and Compounds*; Marks, T. J., Fragala, I. L., Eds.; D Reidel Publishing Company: Dordrecht, Netherlands, 1984; pp 229−276.
(25) Kahn, M. L.; Sutter, J.-P.; Golhen, S.; Guionneau, P.; Ouahab, L.; Kahn, O.; Chasseau, D. *J. Am. Chem. Soc.* **2000**, *122*, 3413−3421.
(26) Costes, J.-P.; Dahan, F.; Dupuis, A.; Laurent, J.-P. *Chem. Eur. J.* **1998**, *4*, 1616−1620.

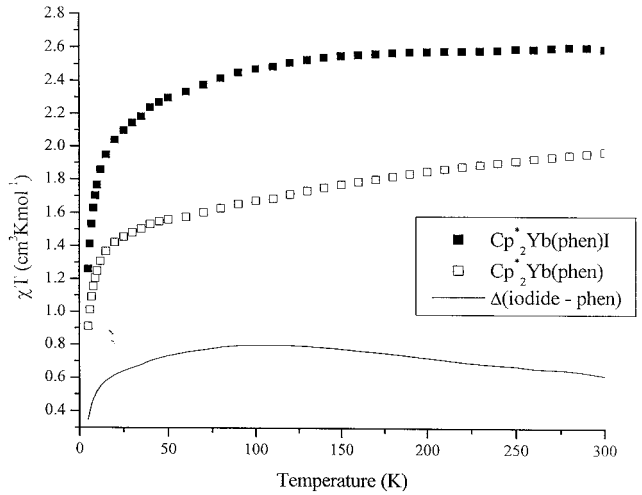

Figure 11. Thermal dependence of χT for $(Me_5C_5)_2Yb(phen)$ and $[(Me_5C_5)_2Yb(phen)]^+[I]^-$ at 40 kG. The solid line represents the difference between the two values of χT.

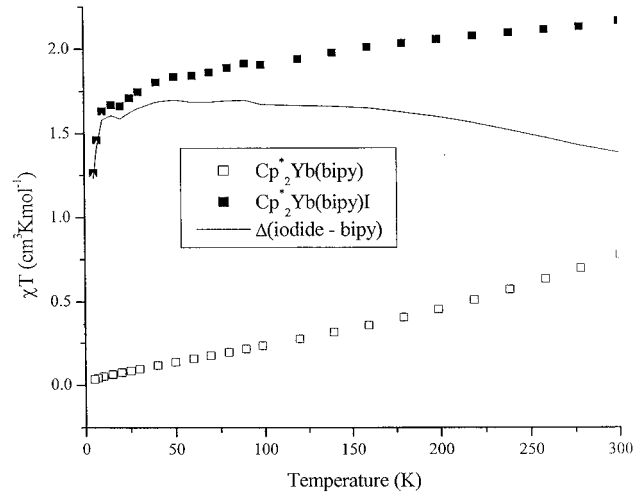

Figure 12. Thermal dependence of χT for $(Me_5C_5)_2Yb(bipy)$ and $[(Me_5C_5)_2Yb(bipy)]^+[I]^-$ at 40 kG. The solid line represents the difference between the two values of χT.

are antiferromagnetically coupled, but the Kahn model does not give a value for the coupling constant. The data for the bipyridyl adducts in Figure 12 leads to a similar conclusion; the salt $[(Me_5C_5)_2Yb(bipy)]^+[I]^-$ has a magnetic susceptibility similar to the phenanthroline salt, as it is also an isolated Yb(III) cation. The χT values for $(Me_5C_5)_2Yb(bipy)$ are very low, but the curve also decreases monotonically from 300 K. Subtraction of the two curves leads to a $\Delta\chi T$ vs T plot with a shape very similar to that observed for the phenanthroline adducts; the value of $\Delta\chi T$ increases slowly with decreasing temperature to a maximum at about 80 K, then drops, indicating that the low magnetic moment of the ground state of $(Me_5C_5)_2Yb(bipy)$ is due to antiferromagnetic coupling between the spin carriers. This is consistent with the field dependence observed (Figure 10).

For the diamagnetic complexes $[1,3\text{-}(Me_3C)_2C_5H_3]_2Yb(bipy)$, $[1,3\text{-}(Me_3Si)_2C_5H_3]_2Yb(bipy)$, and $[1,3\text{-}(Me_3Si)_2C_5H_3]_2Yb(phen)$, the magnetic susceptibilities are expected to be negative, and the measured values are negative for extremely pure samples. The variable-temperature magnetic susceptibility for the only europium adduct prepared in this study, $(Me_5C_5)_2Eu(bipy)$, is as expected for Eu(II) and neutral bipyridyl. As mentioned above, the oxidation potential of $(Me_5C_5)_2Eu$ is significantly lower than that of $(Me_5C_5)_2Yb$,[14] so it is not surprising that the bivalent state is unperturbed by coordination of the bipyridyl ligand. The electronic configuration for Eu(II) is $4f^7$ and an $^8S_{7/2}$ ground state is predicted to have a μ_{eff} of 7.94 μ_B, close to the observed value, Table 1.[20]

Solid-State Measurements: EPR Spectroscopy. The EPR spectrum of $(Me_5C_5)_2Yb(bipy)$ is only observable at temperatures less than 10 K at low microwave power and has a g value of 2.0007. This sort of EPR behavior is atypical of an organic radical and is more nearly like that of a lanthanide ion. Qualitatively, this is consistent with the unpaired electron on bipyridyl coupling with the unpaired electron on Yb, which causes the relaxation time of the bipyridyl electron to decrease dramatically. This makes the EPR signal prone to saturation at high microwave powers, so no further information could be derived.

Solution Measurements: NMR Spectroscopy. The appearance of the proton NMR spectrum of a molecule qualitatively indicates whether the complex is diamagnetic or paramagnetic in solution. The complexes $[1,3\text{-}(Me_3Si)_2C_5H_3]_2Yb(bipy)$ and $[1,3\text{-}(Me_3Si)_2C_5H_3]_2Yb(phen)$ have sharp peaks with chemical shifts in the range 0−10 ppm and resolved coupling patterns in their ^1H NMR spectra, which indicates their diamagnetic nature. The other bipyridyl and phenanthroline complexes have broadened and shifted peaks in their ^1H NMR spectra at 25 °C, consistent with their paramagnetic natures. Surprisingly, the ^1H NMR spectrum of $[1,3\text{-}(Me_3C)_2C_5H_3]_2Yb(bipy)$ indicates that this compound is paramagnetic in solution; the chemical shifts of the protons range from 50 to −1 ppm (see Experimental Section for full details). The solid-state measurements (X-ray crystallography and SQUID) on this molecule point conclusively to diamagnetism, but the ^1H NMR and UV spectra (described below) indicate that at least some (presumably small) proportion of the complex exists in the paramagnetic state in solution.

^1H NMR spectra were collected at temperatures from −80 to +90 °C for each ytterbocene bipyridyl complex to examine the temperature dependence of the chemical shifts. The phenanthroline complexes were insufficiently soluble for the variable-temperature experiments to be useful. A representative plot of δ vs $1/T$ is shown in Figure 13 for $(Me_5C_5)_2Yb(bipy)$. It can be seen that the variation of chemical shift with temperature is not linear, as would be expected for Curie−Weiss behavior. This indicates that some temperature-dependent process occurs in solution.

Addition of free bipyridyl to NMR solutions of the bipyridyl and phenanthroline complexes results in spectra that are the superposition of the spectrum of free bipyridyl and the spectrum of the complex. This behavior is consistent with the hypothesis that on the NMR time scale the complexes do not exchange with added bipyridyl. Similarly, upon addition of 1 equiv of 4,4′-dimethyl-2,2′-bipyridyl (dmb) to a solution of $(Me_5C_5)_2Yb(bipy)$ in an NMR tube, the ^1H spectrum consists of resonances corresponding to the two molecules in the solution. However, after several hours resonances corresponding to $(Me_5C_5)_2Yb(dmb)$ and free

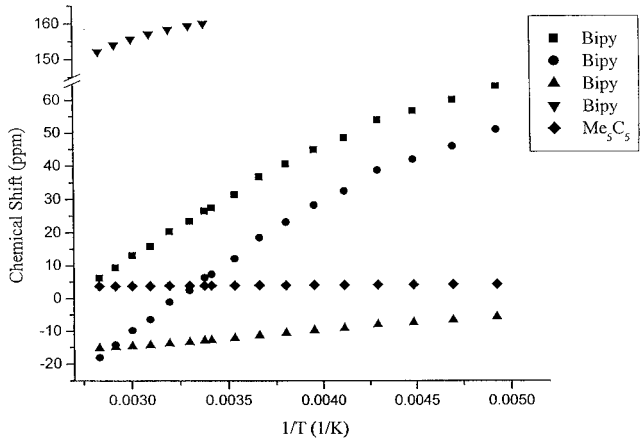

Figure 13. Variable-temperature ^{1}H NMR data for $(Me_5C_5)_2Yb(bipy)$ (tol-d_8): δ vs $1/T$.

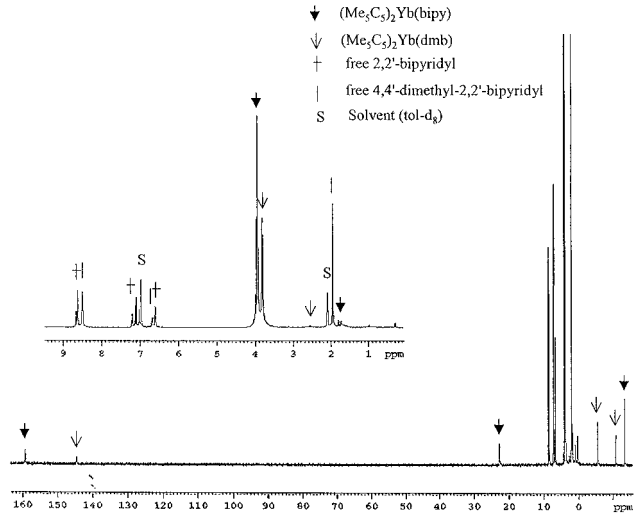

Figure 14. ^{1}H NMR spectrum of $(Me_5C_5)_2Yb(bipy)$ with half an equivalent of dmb at equilibrium (tol-d_8, 20 °C).

bipyridyl can be observed. After approximately 3 days, equilibrium is reached and the solution contains equal amounts of the four compounds. Heating the solution does not change the spectrum after this point. Figure 14 shows the ^{1}H NMR spectrum of a 2:1 mixture of $(Me_5C_5)_2Yb(bipy)$ and dmb after 2 weeks. The paramagnetism of the two ytterbocene complexes is apparent from the shifted and broadened resonances. The equilibrium mixture consists of $(Me_5C_5)_2Yb(bipy)$, $(Me_5C_5)_2Yb(dmb)$, free bipyridyl, and free dmb. Thus, exchange occurs slowly on the chemical time scale.

Similar experiments conducted with the other ytterbocene bipyridyl complexes give widely varying rates of chemical exchange. In the cases of $[1,3\text{-}(Me_3C)_2C_5H_3]_2Yb(bipy)$ and $[1,3\text{-}(Me_3Si)_2C_5H_3]_2Yb(bipy)$, the equilibrium position is reached immediately upon addition of dmb, while the rate for $(Me_4C_5H)_2Yb(bipy)$ is very similar to that for $(Me_5C_5)_2Yb(bipy)$. These results can be compared with a similar experiment conducted on $(Me_5C_5)_2Ca(bipy)$; in that case, exchange with added dmb is also complete upon mixing. The reaction also proceeds in reverse; addition of free bipyridyl to a solution of $(Me_5C_5)_2Yb(dmb)$ results in exchange at a rate very similar to that in the original experiment to reach the same equilibrium position, and the other complexes also exchange ligands in reverse at the same rate as the forward exchange.

Thus, the compounds in which the bipyridyl ligand is reduced exchange ligands much more slowly than the diamagnetic compounds. It is probable that exchange is dissociative, with one arm of the bipyridyl ligand dissociating first, although complete dissociation is also possible given that the base-free bivalent ytterbocenes are known.[27] This implies that the rate-limiting step for exchange in the paramagnetic compounds is the transfer of the electron back from the bipyridyl ligand to the metal, before dissociation of the now neutral ligand occurs. The requirement for rate-determining electron transfer leads to a greater energy barrier to dissociation of a reduced ligand relative to a neutral ligand, so the paramagnetic compounds undergo ligand exchange processes more slowly. The compound $[1,3\text{-}(Me_3C)_2C_5H_3]_2Yb(bipy)$, which is diamagnetic in the solid state but weakly paramagnetic according to its solution NMR spectrum, exchanges rapidly with added dmb, consistent with the electron transfer being less pronounced in this molecule.

The phenanthroline complexes exchange with bipyridyl much more slowly. Addition of 1 equiv of free bipyridyl to a solution of $(Me_5C_5)_2Yb(phen)$, $[1,3\text{-}(Me_3C)_2C_5H_3]_2Yb(phen)$, or $(Me_4C_5H)_2Yb(phen)$ does not result in perceptible exchange even after heating to 60 °C for several weeks. The only phenanthroline complex for which solution exchange with free bipyridyl is observed is the diamagnetic $[1,3\text{-}(Me_3Si)_2C_5H_3]_2Yb(phen)$, and in that case, the exchange is only 20% complete after 2 weeks at room temperature. Thus, phenanthroline is a better ligand for these ytterbocenes than bipyridyl.

Solution Measurements: UV Spectroscopy. The complexes are strongly colored, and their optical spectra were examined. It has been shown that the bipyridyl radical anion has a diagnostic optical spectrum, different from that of the bipyridyl dianion, as expected for a species in which the odd electron is located in a π^* molecular orbital.[28] These characteristic strong absorbances, exemplified by Na(bipy), can be compared with the absorbances of the molecules described here. The UV−vis data for the complexes as toluene solutions are included in Table 5, along with the data for the europocene $(Me_5C_5)_2Eu(bipy)$, the calcocene $(Me_5C_5)_2Ca(bipy)$, and Na(bipy). Figure 15 shows the optical spectra of $(Me_5C_5)_2Yb(bipy)$, $[1,3\text{-}(Me_3Si)_2C_5H_3]_2Yb(bipy)$, and $[1,3\text{-}(Me_3Si)_2C_5H_3]_2Yb(py)_2$. As expected from the previously discussed spectroscopic data, the optical spectra of $(Me_5C_5)_2Yb(bipy)$, $[1,3\text{-}(Me_3C)_2C_5H_3]_2Yb(bipy)$, and $(Me_4C_5H)_2Yb(bipy)$ contain absorbances due to the bipyridyl radical anion, while those of $[1,3\text{-}(Me_3Si)_2C_5H_3]_2Yb(bipy)$, $(Me_5C_5)_2Eu(bipy)$, and $(Me_5C_5)_2Ca(bipy)$ do not. The spectrum of $[1,3\text{-}(Me_3Si)_2C_5H_3]_2Yb(bipy)$ is virtually identical to that of $[1,3\text{-}(Me_3Si)_2C_5H_3]_2Yb(py)_2$, confirming that the bipyridyl ligand is neutral and behaves as two independent pyridine ligands in that complex (Figure 15). The UV−vis spectra qualitatively support the NMR data, as the absorbances indicate the presence of the bipyridyl radical anion in solution, while

(27) Schultz, M.; Burns, C. J.; Schwartz, D. J.; Andersen, R. A. *Organometallics* **2000**, *19*, 781−789.
(28) König, E.; Kremer, S. *Chem. Phys. Lett.* **1970**, *5*, 87−90.

Table 5. Optical Spectra of Bipyridyl and Phenanthroline Complexes (in toluene unless otherwise specified)

complex	λ_{max} in nm ($\epsilon \times 10^{-3}$ in L mol^{-1} cm^{-1})
$(Me_5C_5)_2Yb(bipy)$	1020 (0.88), 890 (2.96), 855 (2.63), 800 (2.37), 505 (5.71), 475 (4.79), 385 (8.98)
$(Me_5C_5)_2Yb(py)_2$	800 (0.47), 441 (0.85)
$(Me_5C_5)_2Yb(phen)$	1007 (0.21), 891 (1.44), 569 (1.29)
$[(Me_5C_5)_2Yb(bipy)]^+[(Me_5C_5)_2YbCl_2]^-$ in CH_2Cl_2	1032 (0.01), 1022 (0.018), 1005 (0.192), 986 (0.036), 977 (0.054), 966 (0.078), 962 (0.055), 956 (0.054), 950 (0.036), 945 (0.02), 927 (0.014), 912 (0.01), 904 (0.015), 900 (0.012), 895 (0.012), 876 (0.012)
$[(Me_5C_5)_2Yb(phen)]^+[I]^-$ in CH_2Cl_2	1006 (0.20), 978 (0.04), 957 (0.04), 570 (0.16)
$[1,3\text{-}(Me_3C)_2C_5H_3]_2Yb(bipy)$	880 (1.00), 845 (1.06), 767 (1.01), 678 (0.76), 488 (1.91), 465 (1.77), 380 (4.19)
$[1,3\text{-}(Me_3C)_2C_5H_3]_2Yb(phen)$	1002 (0.13), 886 (0.53), 539 (1.26), 383 (1.89)
$[1,3\text{-}(Me_3Si)_2C_5H_3]_2Yb(bipy)$	668 (0.41), 392 (1.29)
$[1,3\text{-}(Me_3Si)_2C_5H_3]_2Yb(py)_2$	670 (0.17), 401 (0.24)
$[1,3\text{-}(Me_3Si)_2C_5H_3]_2Yb(phen)$	513 (1.93), 392 (2.04)
$(Me_4C_5H)_2Yb(bipy)$	1035 (0.73), 891 (2.58), 866 (2.36), 801 (2.02), 502 (4.99), 475 (3.94), 383 (9.85)
$(Me_4C_5H)_2Yb(phen)$	1001 (0.28), 891 (1.42), 569 (2.50)
$(Me_5C_5)_2Eu(bipy)$	790 (0.42), 494 (1.62)
$(Me_5C_5)_2Ca(bipy)$	509 (0.97), 365 (0.77)
Na(bipy) in THF	952 (1.3), 833 (1.5), 752 (1.1), 562 (6.5), 532 (6.2), 386 (29.5)

the NMR resonances indicate paramagnetism in the ytterbocene complexes due to electron transfer from ytterbium to the bipyridyl ligand.

Ytterbium(III) complexes have f−f transitions in their optical spectra, which are observed as sharp absorbances from 900 to 1100 nm.[29] These can be observed in the UV spectra of $[(Me_5C_5)_2Yb(bipy)]^+[(Me_5C_5)_2YbCl_2]^-$ as well as $(Me_5C_5)_2Yb(bipy)$ and $(Me_4C_5H)_2Yb(bipy)$, and the phenanthroline adducts of all of the ytterbocenes other than $[1,3\text{-}(Me_3Si)_2C_5H_3]_2Yb$. Illustrative optical spectra of $(Me_5C_5)_2Yb(phen)$ and $[1,3\text{-}(Me_3Si)_2C_5H_3]_2Yb(phen)$ in toluene solution, along with that of $[(Me_5C_5)_2Yb(phen)]^+[I]^-$ in dichloromethane, are shown in Figure 16. The absorptions of phenanthroline radical anion are not as well studied as those of bipyridyl and are not as useful to characterize these adducts. However, once again the diamagnetic complex has spectral data distinctly different from the paramagnetic compounds (Table 5 and Figure 16).

Conclusions

The 1:1 bipyridyl and phenanthroline adducts of the ytterbocenes reported here are not simple diamagnetic metallocene adducts $Cp'_2Yb^{II}(L^0)$, except for the complexes of $[1,3\text{-}(Me_3Si)_2C_5H_3]_2Yb$. They also do not exhibit the predicted magnetism of $Cp'_2Yb^{III}(L^-)$ with noninteracting spins, as is expected for lanthanide complexes with valence f-electrons. According to the model we propose, electron exchange coupling is occurring between the spin carriers in $Cp'_2Yb^{III}(L^-)$ using the methodology described by Kahn.[25] Thus, the ground state is based upon a trivalent ytterbocene fragment. An alternative model is that a chemical equilibrium is occurring between the two discrete electron tautomers, $Cp'_2Yb^{II}(L^0)$ and $Cp'_2Yb^{III}(L^-)$, in the solid state and in solution. The equilibrium constant is temperature dependent, so the concentration of the diamagnetic species must increase with decreasing temperature to fit the measured magnetic susceptibility, which seems unlikely on thermodynamic grounds. To test this hypothesis, a spectroscopic signature of each tautomer must be measured with respect to temperature. However, the physical studies reported here only measure bulk or averaged properties, and no such discrete signatures have been observed. Experimental studies that address this microscopic phenomenon are planned.

The different ytterbocene fragments studied here interact differently with their ligands, depending on the substituents on the cyclopentadienide rings. The Me_3-

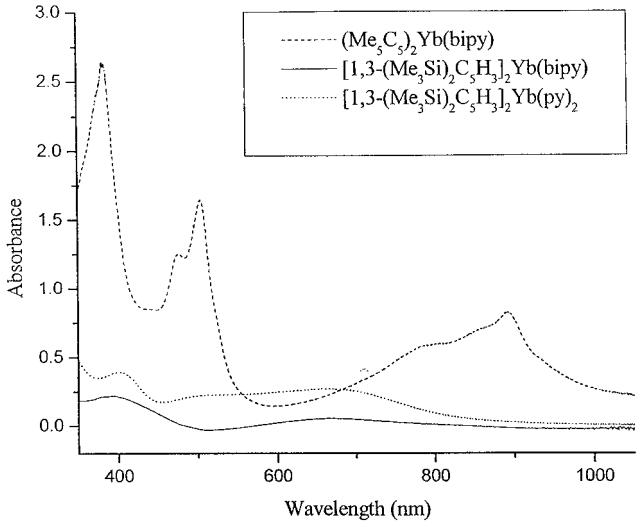

Figure 15. Optical spectra of $(Me_5C_5)_2Yb(bipy)$, $[1,3\text{-}(Me_3Si)_2C_5H_3]_2Yb(bipy)$, and $[1,3\text{-}(Me_3Si)_2C_5H_3]_2Yb(py)_2$ in toluene.

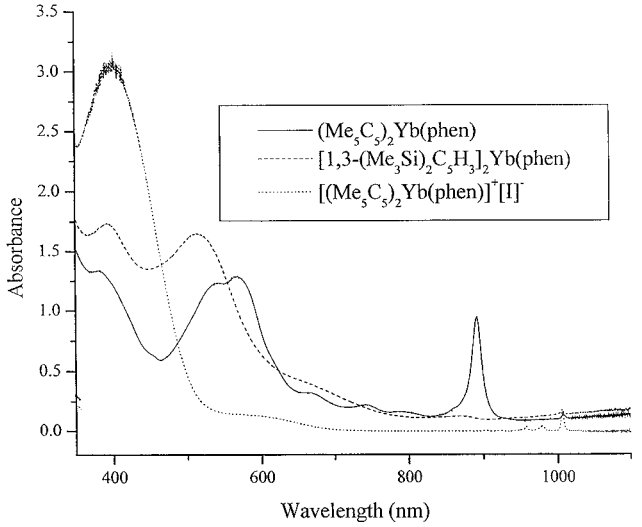

Figure 16. Optical spectra of $(Me_5C_5)_2Yb(phen)$ and $[1,3\text{-}(Me_3Si)_2C_5H_3]_2Yb(phen)$ in toluene and of $[(Me_5C_5)_2Yb(phen)]^+[I]^-$ in dichloromethane.

Si substituents are electron withdrawing, which makes the metal more electropositive, so it does not reduce bipyridyl or phenanthroline. The ytterbocene fragments with penta- and tetramethylcyclopentadienide rings display nearly identical behavior, while the Me_3C substituents on the rings are slightly less electron donating. These conclusions, based on the observed magnetism of the bipyridyl and phenanthroline complexes, are consistent with the character of the Cp'_2Yb fragment as deduced from the CO stretching frequencies of the carbonyl complexes described previously.[30]

Experimental Section

General Comments. All reactions and product manipulations were carried out under dry nitrogen using standard Schlenk and drybox techniques. Dry, oxygen-free solvents were employed throughout. The elemental analyses were performed by the analytical facility at the University of California at Berkeley. The ytterbocene compounds were prepared as previously described: $(Me_5C_5)_2Yb(OEt_2)$,[31] $(Me_5C_5)_2Yb(THF)$,[32] $[1,3\text{-}(Me_3C)_2C_5H_3]_2Yb(OEt_2)$,[27] $[1,3\text{-}(Me_3Si)_2C_5H_3]_2Yb(OEt_2)$,[33] $(Me_4C_5H)_2Yb(OEt_2)$,[27] and $(Me_5C_5)_2YbCl(THF)$,[34] as was the europocene complex $(Me_5C_5)_2Eu(OEt_2)$.[10] 2,2′-Bipyridyl, 4,4′-dimethyl-2,2′-bipyridyl, and 1,10-phenanthroline were purified by sublimation; pyridine was distilled over sodium before use.

$(Me_5C_5)_2Yb(bipy)$. Upon addition of a toluene solution (10 mL) of 2,2′-bipyridyl (0.46 g, 2.95 mmol) to a green solution of $(Me_5C_5)_2Yb(OEt_2)$ (1.53 g, 2.96 mmol) in toluene (25 mL), a dark red-brown solution resulted. The solution was stirred at room temperature for 4 h, and the toluene was removed under vacuum. The resulting brown solid was dissolved in pentane (40 mL), filtered, and concentrated (to 25 mL). Cooling (−10 °C) yielded dark brown prisms in an overall yield of 85% (1.5 g), mp 322−323 °C. Anal. Calcd for $C_{30}H_{38}N_2Yb$: C, 60.1; H, 6.39; N, 4.67. Found: C, 59.9; H, 6.32; N, 4.67. ^{1}H NMR (C_6D_6, 23 °C): δ 160.05 (2H, $\nu_{1/2}$ = 52 Hz, bipy), 26.52 (2H, $\nu_{1/2}$ = 36 Hz, bipy), 6.36 (2H, $\nu_{1/2}$ = 48 Hz, bipy), 3.98 (30H, $\nu_{1/2}$ = 9 Hz, Me_5C_5), −12.87 (2H, $\nu_{1/2}$ = 14 Hz, bipy). ^{13}C NMR (C_6D_6, 23 °C): δ −3.35 (q, *Me*$_5$C$_5$, J_{CH} = 123 Hz), −42.2 (s, Me$_5$*C*$_5$); the bipyridyl resonances were not located.

$[(Me_5C_5)_2Yb(bipy)]^+[I]^-\cdot 1/2CH_2Cl_2$. Bis(pentamethylcyclopentadienyl)ytterbium bipyridyl (0.76 g, 0.0013 mol) in toluene (15 mL), was contacted with AgI (0.30 g, 0.0013 mol) for 24 h. The resultant brown microcrystalline precipitate was isolated by filtration and washed with pentane (2 × 10 mL). The precipitate was then dissolved in CH_2Cl_2 (10 mL), and the CH_2Cl_2 solution was filtered from the silver metal formed in the reaction. Pentane (40 mL) was carefully layered onto the CH_2Cl_2 solution, and diffusive mixing of the solvents at room temperature resulted in quantitative yield of red-brown plates which cocrystallize with half a molecule of dichloromethane per ytterbium center, mp 125−130° (dec). Anal. Calcd for $C_{30.5}H_{39}ICIN_2Yb$: C, 47.6; H, 5.11; I, 16.5; N, 3.64. Found: C, 47.9; H, 5.23; I, 16.7; N, 3.63.

Reduction of $[(Me_5C_5)_2Yb(bipy)]^+[I]^-$. Bis(pentamethylcyclopentadienyl)ytterbium(III) bipyridyliodide (0.17 g, 0.23 mmol) in THF (50 mL) was exposed to excess sodium amalgam. The reaction turned dark brown, and the reaction mixture was stirred for 12 h. The THF was then removed under reduced pressure, and the brown residue was extracted into hexane (30 mL) and filtered. The hexane was removed under reduced pressure to yield a brown microcrystalline solid, which was identified as $(Me_5C_5)_2Yb(bipy)$ by its infrared spectrum and melting point, which were identical to those of the sample prepared from $(Me_5C_5)_2Yb(OEt_2)$ and 2,2′-bipyridyl (described above).

$[(Me_5C_5)_2Yb(bipy)]^+[(Me_5C_5)_2YbCl_2]^-$. The THF adduct of $(Me_5C_5)_2YbCl$ (0.23 g, 0.42 mmol) was dissolved in 20 mL of toluene and then added to a solution of 2,2′-bipyridyl (0.03 g, 0.19 mmol) in toluene (10 mL). A brown microcrystalline precipitate formed immediately. After 20 min of stirring, the supernatant was discarded; the solid was washed in toluene (2 × 10 mL) and then dissolved in CH_2Cl_2 (5 mL). Pentane (50 mL) was carefully layered onto the CH_2Cl_2 solution; after 3 days the solution had diffused to give a quantitative yield, mp 264−266° (dec). Anal. Calcd for $C_{50}H_{68}Cl_2N_2Yb$: C, 53.9; H, 6.15; Cl, 6.36; N, 2.51. Found: C, 53.85; H, 6.07; Cl, 5.55; N, 2.50. The compound has a conductivity of 11.2 Ω^{-1} cm^2 mol^{-1} in CH_3CN solution. ^{1}H NMR ($CDCl_3$, 28 °C): δ 58.00 (2H, bipy), 15.82 (2H, bipy), 3.23 (30H, Me_5C_5), 1.43 (30H, Me_5C_5), −1.91 (2H, bipy). The remaining proton of the bipyridyl was not located.

$(Me_5C_5)_2Yb(dmb)$. 4,4′-Dimethyl-2,2′-bipyridyl (0.28 g, 1.6 mmol) and $(Me_5C_5)_2Yb(OEt_2)$ (0.80 g, 1.6 mmol) were weighed into a Schlenk flask and dissolved in toluene (40 mL) with stirring. The brown solution was filtered, and the filtrate was concentrated to 20 mL. Cooling at −10 °C overnight produced large brown crystals. Yield: 0.67 g, 69%, mp > 300 °C. Anal. Calcd for $C_{32}H_{42}N_2Yb$: C, 61.2; H, 6.74; N, 4.46. Found: C, 60.8; H, 6.72; N, 4.42. ^{1}H NMR (C_6D_6, 32 °C): δ 143.0 (2H, $\nu_{1/2}$ = 84 Hz, dmb), 3.8 (30H, $\nu_{1/2}$ = 15 Hz, Me_5C_5), 2.5 (2H, $\nu_{1/2}$ = 60 Hz, dmb) −6.1 (6H, $\nu_{1/2}$ = 30 Hz, Me_2), −10.5 (2H, $\nu_{1/2}$ = 14 Hz).

$(Me_5C_5)_2Yb(phen)$. A procedure similar to that used to prepare $(Me_5C_5)_2Yb(dmb)$ was followed, yielding an insoluble dark blue microcrystalline powder. Yield: 85%, mp 297−300 °C. Anal. Calcd for $C_{32}H_{38}N_2Yb$: C, 61.6; H, 6.14; N, 4.49. Found: C, 61.6; H, 6.18; N, 4.42. ^{1}H NMR (C_7D_8, 23 °C): δ 4.14 ($\nu_{1/2}$ = 12.5 Hz, Me_5C_5). The phenanthroline resonances were not observed.

$(Me_5C_5)_2YbI\cdot thf$. Method 1. The complex $(Me_5C_5)_2Yb(THF)$ (0.58 g, 1.12 mmol) in toluene (25 mL) was added to silver iodide (0.27 g, 1.15 mmol), and the mixture was stirred for 14 h. The violet solution was filtered, concentrated to 8 mL under reduced pressure, and cooled (−10 °C). Red crystals were obtained in 60% yield (0.43 g). When heated in a sealed capillary, the compound decomposes (turns brown) at 130 °C. Anal. Calcd for $C_{24}H_{38}OIYb$: C, 44.9; H, 5.96. Found: C, 45.1; H, 6.10. IR (Nujol): 2723 w, 1344 m, 1248 w, 1178 w, 1039 w sh, 1012 s, 956 w, 925 w, 914 w sh, 860 s, 841 w sh, 730 m, 697 w, 676 w, 595 m, 388 m, 308 s cm^{-1}.

Method 2. $(Me_5C_5)_2Yb(OEt_2)$ (1.15 g, 2.22 mmol) was weighed into a Schlenk flask and dissolved in toluene (40 mL). A solution of iodine (0.30 g, 1.2 mmol) in 20 mL of toluene was added with vigorous stirring. The solution changed color to deep blue-green with precipitation of a bright green solid. After stirring for 1 h, the solvent was removed and the insoluble residue was washed with hexane. The powder was then dissolved in THF to give a brilliant blue solution. On slight warming, the color of the solution changed irreversibly to deep gold. Concentration and cooling produced a small quantity of red crystals. Yield: 0.21 g (14%). The melting point and infrared spectrum were identical to those obtained for the compound obtained by method 1.

$[(Me_5C_5)_2Yb(phen)]^+[I]^-\cdot(CH_2Cl_2)_{1-2}$. The trivalent iodide $(Me_5C_5)_2YbI$ (0.55 g, 0.96 mmol) was weighed into a Schlenk flask equipped with a magnetic stirrer. 1,10-Phenanthroline (0.17 g, 0.96 mmol) was added, followed by toluene (60 mL). The slurry was stirred overnight, during which time the color

(29) Thomas, A. C. Ph.D. Thesis; University of Wisconsin−Madison: Madison, WI, 1985.
(30) Schultz, M.; Burns, C. J.; Schwartz, D. J.; Andersen, R. A. *Organometallics* **2001**, *20*, 5690−5699.
(31) Tilley, T. D.; Boncella, J. M.; Berg, D. J.; Burns, C. J.; Andersen, R. A. *Inorg. Synth.* **1990**, *27*, 146−149.
(32) Tilley, T. D.; Andersen, R. A.; Spencer, B.; Ruben, H.; Zalkin, A.; Templeton, D. H. *Inorg. Chem.* **1980**, *19*, 2999−3003.
(33) Hitchcock, P. B.; Howard, J. A. K.; Lappert, M. F.; Prashar, S. *J. Organomet. Chem.* **1992**, *437*, 177−189.
(34) Tilley, T. D.; Andersen, R. A. *Inorg. Chem.* **1981**, *20*, 3267−3270.

changed from green to red. The supernatant was discarded, and the product was extracted into methylene chloride (50 mL). Cooling to −80 °C led to the formation of red-brown crystals, which are found by microanalysis and X-ray crystallography to contain between one and two molecules of methylene chloride of crystallization, mp 173−177 °C. Anal. Calcd for $C_{33.5}H_{41}YbCl_3N_2I$: C, 45.8; H, 4.67; N, 3.19. Found: C, 46.7; H, 4.80; N, 3.32. ^{1}H NMR (CD_2Cl_2, 23 °C): δ 52.37 (2H, $\nu_{1/2}$ = 25 Hz, phen), 9.42 (2H, $\nu_{1/2}$ = 16 Hz, phen), 5.32 (2H, $\nu_{1/2}$ = 5 Hz, phen), 3.80 (30H, $\nu_{1/2}$ = 50 Hz, Me_5C_5), −2.56 (2H, $\nu_{1/2}$ = 20 Hz, phen). IR (Nujol): 1622 (w), 1518 (w), 1460 (s), 1415 (m), 1377 (s), 1273 (w), 855 (m), 728 (s).

[1,3-(Me_3C)$_2$$C_5H_3$]$_2$Yb(bipy). A procedure similar to that used to prepare (Me_5C_5)$_2$Yb(dmb) was followed, yielding a blue crystalline product in 90% yield. The crystal that was studied by X-ray diffraction had one molecule of toluene per ytterbocene unit; however, this was removed upon exposure to dynamic vacuum, mp 278−280 °C. Anal. Calcd for $C_{36}H_{50}N_2Yb$: C, 63.2; H, 7.37; N, 4.10. Found: C, 64.0; H, 7.34; N, 3.74. ^{1}H NMR (C_7D_8, 23 °C): δ 49.53 (2H, $\nu_{1/2}$ = 30 Hz, bipy), 18.49 (2H, $\nu_{1/2}$ = 25 Hz, bipy), 10.58 (2H, $\nu_{1/2}$ = 22 Hz, bipy), 1.96 (36H, $\nu_{1/2}$ = 18 Hz, Me_3C), 1.00 (2H, $\nu_{1/2}$ = 10 Hz, bipy), 0.84 (4H, $\nu_{1/2}$ = 75 Hz, C_5H_3), −1.00 (2H, $\nu_{1/2}$ = 11 Hz, C_5H_3).

[1,3-(Me_3C)$_2$$C_5H_3$]$_2$Yb(phen)·1/2toluene. A procedure similar to that used to prepare (Me_5C_5)$_2$Yb(dmb) was followed, yielding a dark blue microcrystalline product in quantitative yield which cocrystallizes with half a molecule of toluene per ytterbocene unit, mp 224−228 °C. Anal. Calcd for $C_{41.5}H_{54}N_2Yb$: C, 66.1; H, 7.22; N, 3.72. Found: C, 66.0; H, 7.07; N, 3.99. ^{1}H NMR (C_6D_6, 23 °C): δ 48.19 (2H, $\nu_{1/2}$ = 16 Hz, phen), 22.22 (2H, $\nu_{1/2}$ = 20 Hz, phen), 11.27 (2H, $\nu_{1/2}$ = 14 Hz, phen), 5.04 (2H, $\nu_{1/2}$ = 4 Hz, C_5H_3), 2.07 (36H, $\nu_{1/2}$ = 9 Hz Hz, Me_3C), 1.14 (4H, $\nu_{1/2}$ = 8 Hz, C_5H_3), −0.77 (2H, $\nu_{1/2}$ = 10 Hz, phen).

[1,3-(Me_3Si)$_2$$C_5H_3$]$_2$Yb(bipy). A procedure similar to that used to prepare (Me_5C_5)$_2$Yb(dmb) was followed, yielding a blue-green crystalline product in 90% yield, mp 208−212 °C. Anal. Calcd for $C_{32}H_{50}N_2Si_4Yb$: C, 51.4; H, 6.74, N, 3.74. Found: C, 50.5; H, 6.72; N, 3.58. ^{1}H NMR (C_6D_6, 23 °C): δ 13.20 (d, J = 4.5 Hz, 2H, bipy), 9.63 (t, J = 7.5 Hz, 2H, bipy), 7.72 (t, J = 5.4 Hz, 2H, bipy), 6.34 (t, J = 8.1 Hz, 2H, bipy), 6.31 (d, J = 1.6 Hz, 4H, C_5H_3), 5.07 (t, J = 2 Hz, 2H, C_5H_3), 0.26 (s, 36H, Me_3Si).

[1,3-(Me_3Si)$_2$$C_5H_3$]$_2$Yb(dmb)·toluene. A procedure similar to that used to prepare (Me_5C_5)$_2$Yb(dmb) was followed, yielding a blue-green crystalline product in 90% yield that cocrystallizes with one molecule of toluene, mp 190−192 °C. Anal. Calcd for $C_{41}H_{62}N_2Si_4Yb$: C, 56.7; H, 7.20; N, 3.23. Found: C, 56.4; H, 6.90, N, 3.15. ^{1}H NMR (C_6D_6, 23 °C): δ 9.68 (d, J = 5.2 Hz, 2H, dmb ring), 7.10 (m, 5H, toluene), 6.99 (s, 2H, dmb ring), 6.83 (d, J = 5.0 Hz, 2H, dmb ring), 6.68 (d, J = 1.8 Hz, 4H, C_5H_3), 5.78 (t, J = 1.6 Hz, 2H, C_5H_3), 2.10 (s, 3H, toluene), 0.99 (s, 6H, Me of dmb), 0.24 (s, 36H, Me_3Si).

[1,3-(Me_3Si)$_2$$C_5H_3$]$_2$Yb(phen). A procedure similar to that used to prepare (Me_5C_5)$_2$Yb(dmb) was followed, yielding a red crystalline product in quantitative yield, mp 216−218 °C. Anal. Calcd for $C_{34}H_{50}N_2Si_4Yb$: C, 52.9; H, 6.53; N, 3.63. Found: C, 53.3; H, 6.50; N, 3.63. ^{1}H NMR (C_6D_6, 23 °C): δ 15.01 (d, J = 4 Hz, 2H, phen), 12.03 (d, J = 7.5 Hz, 2H, phen), 8.04 (dd, J = 8 Hz, J = 4.5 Hz, 2H, phen), 6.82 (s, 2H, phen), 6.22 (d, J = 1 Hz, 4H, C_5H_3), 5.05 (t, J = 1.5 Hz, 2H, C_5H_3), 0.17 (s, 36H, Me_3Si).

[1,3-(Me_3Si)$_2$$C_5H_3$]$_2$Yb(py)$_2$. Pyridine (0.15 mL, 1.8 mmol) was added with stirring to a green toluene solution of [1,3-(Me_3Si)$_2$$C_5H_3$]$_2$Yb($OEt_2$) (0.61 g, 0.9 mmol). The solution immediately became deep blue. After filtration, the solution was concentrated and cooled to −30 °C to give a deep blue microcrystalline powder in 90% yield, mp 145−150 °C. Anal. Calcd for $C_{32}H_{52}N_2Si_4Yb$: C, 51.2; H, 6.99; N, 3.73. Found: C, 50.4; H, 7.01; N, 3.50. ^{1}H NMR (C_6D_6, 23 °C): δ 8.51 (br, 4H, py), 6.96 (t, J = 6 Hz, 2H, py), 6.83 (d, J = 1.9 Hz, 4H, C_5H_3), 6.61 (t, J = 4 Hz, 4H, py), 6.28 (t, J = 1.9 Hz, 2H, C_5H_3), 0.24 (s, 36H, Me_3Si).

(Me_4C_5H)$_2$Yb(bipy). A procedure similar to that used to prepare (Me_5C_5)$_2$Yb(dmb) was followed, yielding a red-brown crystalline product in quantitative yield, mp 285−288 °C. Anal. Calcd for $C_{28}H_{34}N_2Yb$: C, 58.8; H, 6.00; N, 4.90. Found: C, 57.9; H, 5.86; N, 4.93. ^{1}H NMR (C_6D_6, 23 °C): δ 173.7 (2H, $\nu_{1/2}$ = 60 Hz, bipy), 20.9 (12H, $\nu_{1/2}$ = 10 Hz, Me_4C_5), 20.5 (2H, $\nu_{1/2}$ = 25 Hz, bipy), −1.4 (2H, $\nu_{1/2}$ = 37 Hz, bipy), −3.2 (12H, $\nu_{1/2}$ = 9 Hz, Me_4C_5), −17.0 (2H, $\nu_{1/2}$ = 8 Hz, C_5H), −45.3 (2H, $\nu_{1/2}$ = 30 Hz, bipy).

(Me_4C_5H)$_2$Yb(phen). A procedure similar to that used to prepare (Me_5C_5)$_2$Yb(dmb) was followed, yielding a deep blue microcrystalline product in quantitative yield, mp 230−233 °C. Anal. Calcd for $C_{30}H_{34}N_2Yb$: C, 60.5; H, 5.75; N, 4.70. Found: C, 60.3; H, 5.87; N, 4.56. ^{1}H NMR (C_6D_6, 23 °C): δ 20.32 (12H, Me_4C_5), −3.00 (12H, Me_4C_5), −40.2 (2H, C_5H); the phenanthroline resonances were not observed.

(Me_5C_5)$_2$Eu(bipy). This complex was prepared by addition of 2,2′-bipyridyl (0.31 g, 2.0 mmol) in toluene (20 mL) to (Me_5C_5)$_2$Eu(OEt_2) (1.03 g, 2.0 mmol) in toluene (15 mL). After stirring for 3 h and removing the solvent under reduced pressure, the resulting dark brown solid was crystallized from THF (−70 °C). Yield: 1.05 g (91%), mp 328−332 °C. Anal. Calcd for $C_{30}H_{38}N_2Eu$: C, 62.3; H, 6.62; N, 4.84. Found: C, 62.1; H, 6.58; N, 4.70. ^{1}H NMR (C_6D_6, 23 °C): δ 4.8 ($\nu_{1/2}$ = 1500 Hz); the bipyridyl protons were not observed.

Crystallographic Studies. All relevant data collection and structure solution parameters are shown in Table 4.

General Procedure for (Me_5C_5)$_2$Yb(bipy) and [(Me_5C_5)$_2$Yb(bipy)]$^+$[(Me_5C_5)$_2$$YbCl_2$]$^-$. A crystal of appropriate dimensions was mounted in a thin-walled quartz capillary which was flame sealed. Preliminary precession photographs indicated the Laue symmetry of the crystal, which was then transferred to an Enraf-Nonius CAD-4 diffractometer and centered in the beam, and data were collected at room temperature. Automatic peak search and indexing procedures revealed the unit cell parameters and the space group. The raw intensity data were converted to structure factor amplitudes and their esd's by correction for background, scan speed, and Lorentz and polarization effects.[35] There was no indication of crystal decomposition during collection. An absorption correction based on crystal shape and dimensions and an internal Gaussian grid of points was applied after solution of the structure but before anisotropic refinement. Analysis of Patterson maps yielded the positions of the heavy atoms. All other non-hydrogen atoms were located via standard Fourier and least-squares techniques.

(Me_5C_5)$_2$Yb(bipy). The maximum and minimum transmission factors were 0.66 and 0.56, respectively. In the final refinement, the two unique molecules in the asymmetric unit were refined in separate blocks, with the scale factor refined separately for each block. Hydrogen atoms were not placed. There is gross thermal motion of the cyclopentadienide rings in the plane of those rings, but this should not affect the accuracy of other atomic positions.

[(Me_5C_5)$_2$Yb(bipy)]$^+$[(Me_5C_5)$_2$$YbCl_2$]$^-$. The maximum and minimum transmission factors were 0.622 and 0.509, respectively. Hydrogen atoms were located and placed in idealized positions having fixed thermal parameters and were included in structure factor calculations but were not refined. A secondary extinction correction was applied.

General Procedure for [1,3-(Me_3C)$_2$$C_5H_3$]$_2$Yb(bipy)·toluene, [1,3-($Me_3Si$)$_2$$C_5H_3$]$_2$Yb(phen), and [($Me_5C_5$)$_2$Yb(phen)]$^+$[I]$^-$·$CH_2Cl_2$. A crystal of appropriate dimensions was mounted on a glass fiber using Paratone N hydrocarbon oil. All measurements were made on a Siemens SMART diffractometer.[36] Cell constants and an orientation matrix were

(35) *Structure Determination User's Guide*; BA Frenz and Associates, Inc: College Station, TX, 1985.

obtained from a least-squares refinement of the measured positions of reflections with $I > 10\sigma$ (unless otherwise specified) to give the unit cell. The systematic absences uniquely determined the space group in each case. An arbitrary hemisphere of data was collected at low temperature using the ω scan technique with 0.3° scans counted for 20 s per frame. Data were integrated using SAINT[37] and corrected for Lorentz and polarization effects. The data were analyzed for agreement and absorption using XPREP,[38] and an empirical absorption correction was applied based on comparison of redundant and equivalent reflections. After solution of the structure, it was expanded using Fourier techniques,[39] and the non-hydrogen atoms were refined anisotropically. Hydrogen atoms were included in calculated positions but not refined.

[1,3-(Me$_3$C)$_2$C$_5$H$_3$]$_2$Yb(bipy)·toluene. The location of the ytterbium atom was determined by Patterson methods.[40] The asymmetric unit consists of half the molecule as the ytterbium atom lies on a 2-fold axis. After the ytterbocene molecule had been refined, peaks were observed in the difference map corresponding to 1 equiv of toluene of crystallization. The toluene molecule lies on a 222 special position, and the methyl group is disordered over four symmetry-equivalent positions. This has been modeled with 0.25 occupancy for that atom (C(21)) which was refined isotropically. No hydrogen atoms were included for the toluene molecule.

[1,3-(Me$_3$Si)$_2$C$_5$H$_3$]$_2$Yb(phen). The structure was solved by direct methods.[41]

[(Me$_5$C$_5$)$_2$Yb(phen)]$^+$[I]$^-$·CH$_2$Cl$_2$. Cell constants and an orientation matrix were obtained from a least-squares refinement of the measured positions of reflections with $I > 25\sigma$ to give the unit cell. The structure was then solved by direct methods.[41] After location and refinement of the ytterbocene molecule, peaks were observed in the difference map corresponding to two molecules of methylene chloride of crystallization per ytterbocene unit. Further refinement led to large thermal parameters for the atoms of one of these molecules, so the occupancy of that molecule was refined (refined value 0.62).

Acknowledgment. This work was partially supported by the Director, Office of Energy Research, Office of Basic Energy Sciences, Chemical Sciences Division of the U.S. Department of Energy under Contract No. DE-AC03-76SF00098. We thank Dr. Fred Hollander for assistance with the crystallography and NSERC (Canada) for a fellowship (D.J.B.).

Supporting Information Available: Plots of $1/\chi$ vs T and μ vs T for the paramagnetic compounds are available, as well as atomic positions and anisotropic thermal parameters, tables of bond lengths and angles, and least squares planes for each crystal structure. This material is available free of charge via the Internet at http://pubs.acs.org. Structure factor tables are available from the authors.

OM010661K

(36) *SMART Area-Detection Software Package*; Siemens Industrial Automation, Inc: Madison, WI, 1995.
(37) *SAINT*; 4.024 ed.; Siemens Industrial Automation, Inc: Madison, WI, 1995.
(38) Sheldrick, G. M. *XPREP*; 5.03 ed.; Siemens Industrial Automation, Inc: Madison, WI, 1995.
(39) Beurskens, P. T.; Admiraal, G.; Beurskens, G.; Bosman, W. P.; de Gelder, R.; Israel, R.; Smits, J. M. M. *The DIRDIF-94 Program System*; University of Nijmegen: Nijmegen, The Netherlands, 1994.
(40) Sheldrick, G. M. *SHELXTL Crystal Structure Determination Package*; Siemens Industrial Automation, Inc: Madison, WI, 1981.
(41) Altomare, A.; Cascarano, M.; Giacovazzo, C.; Guagliardi, A. *J. Appl. Crystallogr.* **1993**, *26*, 343−350.